



Our study focused on the spectral and temporal characteristics of the intracellular fluorescence excited at 365 nm, which is dominated by the NADH signal.<sup>3,9</sup> The results of the fitting analysis in three typical wavelength bands and the full band of 16 channels are summarized in Table 1. The fittings were based on the experimental data measured from ten samples. As can be seen, a dual-exponential function provides an excellent description of the intracellular fluorescence decay process, as indicated by the high determination coefficient,  $r^2$ . The short and long lifetimes are stable at all emission spectral bands from 400 to 600 nm and comparable with the decay times of free NADH ( $\sim 0.4$  ns) and protein-bound NADH ( $>1$  ns), respectively.<sup>4,10</sup> Moreover, they are consistent with those measured from the nonkeratinized epithelial tissue.<sup>5</sup>

To develop further understanding of the information carried in two lifetime components, we constructed and analyzed the decay-associated spectra (DAS) of short and long lifetime components. In detail, the short and long lifetime DAS were formed with the values of  $A_1\tau_1$  and  $A_2\tau_2$  calculated from the signals recorded at 16 wavelength bands, respectively. The DAS for the fluorescence signals measured from SiHa and Ect1 samples are shown in Fig. 2. The peaks of short lifetime DAS from SiHa and Ect1 are at  $\sim 452$  nm. The long lifetime DAS are almost identical and have an  $\sim 13$  nm blueshift from the short lifetime DAS. It is known that enzyme binding induces the blueshift of NADH fluorescence.<sup>3,11</sup> For comparison, we measured the fluorescence spectra of a pure 500  $\mu$ M NADH solution (N8129, Sigma-Aldrich) and a 250  $\mu$ M NADH solution mixed 1:1 with 1000 unit/ml lactate dehydrogenase (LDH, L3916, Sigma-Aldrich), one of several cellular enzymes that can bind with NADH. The results are displayed together with the short and long lifetime DAS of cells in Fig. 2. As can be seen, the LDH binding induces a 13 nm blueshift from the free NADH fluorescence similar to the spectral shifts between long and short lifetime DAS measured from SiHa and Ect1 cell samples. Because free NADH does not contribute to the long lifetime component, the long lifetime DAS should represent the spectra of bound NADH in cells except the possible interference from FAD fluorescence beyond 520 nm.<sup>3,9</sup> Though the short lifetime DAS have the signal peaks and line

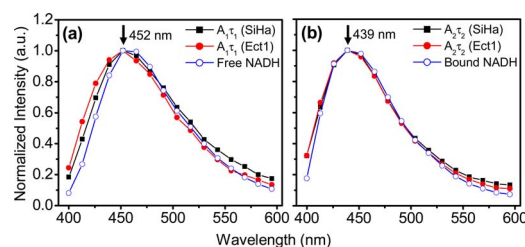


Fig. 2. (Color online) (a) Normalized short lifetime DAS of SiHa and Ect1 cells and the fluorescence spectrum of pure NADH. (b) Normalized long lifetime DAS of SiHa and Ect1 cells and the fluorescence spectrum of LDH-bound NADH.

shapes close to the free NADH signal, the small blueshifts from the free NADH cause little shoulders in the wavelength range from 400 to 450 nm as shown in Fig. 2(a). This indicates some contribution of bound NADH to the short lifetime component because the fluorescence decay of bound NADH is usually multiexponential with short lifetime components comparable with that of free NADH.<sup>12,13</sup> Therefore the short lifetime component could be mainly determined by free NADH with certain interference of bound NADH.

To investigate the correlation of two lifetime components with the cellular metabolic state, the fluorescence time decay was measured from SiHa and Ect1 samples before and after being treated with the mitochondrial inhibitor sodium cyanide (NaCN) and uncoupler carbonyl cyanide-3-chloro-phenylhydrazine (CCCP).<sup>9</sup> With the excitation at 365 nm, no obvious changes of short and long lifetimes were observed after with NaCN and CCCP. The ratios of the amplitudes of two lifetime components ( $A_1/A_2$ ) as a function of wavelength band are displayed in Figs. 3(a) and 3(b). As can be seen, the  $A_1/A_2$ -ratio values increase with treatment from NaCN and decreased with treatment from CCCP, indicating that the  $A_1/A_2$  ratio is a sensitive indicator for cell metabolism. The result is consistent with the study in other cell samples.<sup>14</sup> In addition, it was found that the  $A_1/A_2$  ratio generally increases with the increase of wavelength (400–530 nm) because of the blueshift of the bound NADH fluorescence with respect to the free NADH fluorescence. Because of the contribution of bound NADH to the short lifetime component in the wavelength range from 400 to 450 nm, the  $A_1/A_2$  ratio measured in the long wavelength region (e.g., 460–600 nm) should produce a more accurate estimation of the free–bound NADH ratio. Furthermore, we compared the  $A_1/A_2$  ratios between SiHa and Ect1 cell samples. The comparison shown in Fig. 3(c) demonstrates that the  $A_1/A_2$  ratios in Ect1 cells are significantly lower than in SiHa cells. The two types of cells established from the same tissue site can be clearly differentiated based on the measurement of time-resolved cellular fluorescence. The higher  $A_1/A_2$  ratios in SiHa cells is in accordance with the findings of Galeotti *et al.* on the loss of binding sites for NADH in malignant cells causing an increase of free NADH concentration.<sup>2</sup> The loss of binding sites for NADH in malignant cells could be related to the anaerobic metabolism in neoplastic cells.<sup>15</sup>

**Table 1. Fitting Analysis of Cellular Fluorescence Excited at 365 nm**

Cell Line	$\lambda$ ( $\pm 5$ nm)	$\tau_1$ (ns)	$\tau_2$ (ns)	$r^2$
SiHa	439 nm	$0.42 \pm 0.03$	$3.71 \pm 0.17$	$0.997 \pm 0.001$
	478 nm	$0.43 \pm 0.03$	$3.60 \pm 0.28$	$0.997 \pm 0.001$
	530 nm	$0.41 \pm 0.04$	$3.29 \pm 0.25$	$0.992 \pm 0.003$
	Full	$0.42 \pm 0.05$	$3.59 \pm 0.38$	$0.990 \pm 0.012$
Ect1	439 nm	$0.44 \pm 0.01$	$3.62 \pm 0.14$	$0.997 \pm 0.001$
	478 nm	$0.46 \pm 0.02$	$3.48 \pm 0.13$	$0.998 \pm 0.001$
	530 nm	$0.47 \pm 0.03$	$3.41 \pm 0.18$	$0.995 \pm 0.003$
	Full	$0.45 \pm 0.04$	$3.55 \pm 0.30$	$0.995 \pm 0.009$

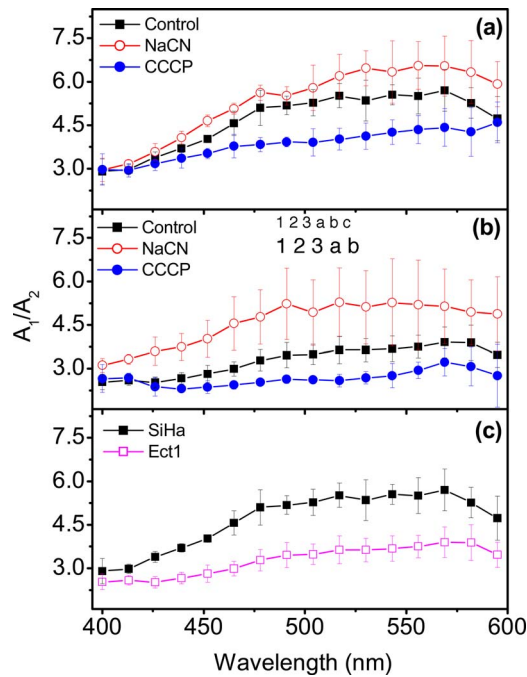


Fig. 3. (Color online) Variation of the  $A_1/A_2$  ratio as a function of wavelength. (a) SiHa cells treated before and after with NaCN and CCCP. (b) Ect1 cells treated before and after with NaCN and CCCP. (c) Comparison between SiHa and Ect1 cells.

**Table 2. Analysis of Time-Resolved Fluorescence Measured from SiHa Cells with an Excitation Range from 365 to 405 nm**

Excitation		365 nm	385 nm	405 nm
Control	$\tau_1$ (ns)	0.42±0.03	0.38±0.02	0.37±0.03
	$\tau_2$ (ns)	3.60±0.13	3.22±0.10	3.82±0.02
	$A_1/A_2$	4.02±0.13	3.88±0.18	3.71±0.11
NaCN	$A_1/A_2$	4.65±0.20	4.26±0.19	3.78±0.15
	Increase	16%	10%	2%
CCCP	$A_1/A_2$	3.52±0.17	3.53±0.19	3.64±0.15
	Decrease	13%	9%	2%

Finally, we investigated the effect of excitation wavelength on the time-resolved fluorescence sensing of cell metabolism. We tuned the laser wavelength in the range from 365 to 405 nm to excite the fluorescence signals from SiHa samples before and after being treated with NaCN and CCCP. As listed in Table 2, the short lifetime ( $\tau_1$ ) and the long lifetime ( $\tau_2$ ) are different at three typical excitation wavelengths at 365, 385, and 405 nm. More importantly, the NaCN- and CCCP-induced changes of the  $A_1/A_2$  ratio are highly dependent on the excitation wavelength. Here, the fluorescence in the wavelength band from 447 to 457 nm was chosen to calculate the  $A_1/A_2$  ratio because the signal in this band is dominated by NADH signals.<sup>3,5,9</sup> After cells were treated with NaCN and CCCP, the changes of the  $A_1/A_2$  ratio decrease with the increase of excitation wavelength, meaning that the time-resolved fluorescence becomes less sensitive to the cell metabolic activity at long excitation wave-

length. In particular, the contrast in the  $A_1/A_2$  ratio before and after treatment with NaCN and CCCP almost disappears at the 405 nm excitation. This may be caused by the increased interference from the FAD fluorescence because FAD and NADH signals reach the balanced level at 405 nm excitation.<sup>5</sup> Though free FAD fluorescence has a long lifetime, the decay of bound FAD fluorescence is multiexponential including a short lifetime component.<sup>10</sup> Therefore FAD fluorescence contributes to both lifetime components and affects the  $A_1/A_2$  ratio.

In conclusion, the decay of cellular fluorescence can be well described by a dual-exponential function. The long lifetime component carries the information of bound NADH, and the short lifetime component is mainly determined by free NADH with certain interference from bound NADH. We demonstrate that the  $A_1/A_2$  ratio can clearly differentiate SiHa cells from Ect1 cells, the cell lines established from cancerous and normal epithelial tissues at the same site, the ectocervix. In future work, we will study the time-resolved fluorescence of neoplastic and normal cell lines and further explore the method to detect neoplastic growth in the epithelium using the combined depth- and time-resolved fluorescence technique.

The authors gratefully acknowledge the support of the Hong Kong Research Grants Council through the grants HKUST6025/02M and HKUST6408/05M. J. Y. Qu's e-mail address is [eequ@ust.hk](mailto:eequ@ust.hk).

## References

1. B. Chance, P. Cohen, F. Jobsis, and B. Schoener, *Science* **137**, 499 (1962).
2. T. Galeotti, G. D. V. VanRossum, D. H. Mayer, and B. Chance, *Eur. J. Biochem.* **17**, 485 (1970).
3. J. M. Salmon, E. Kohen, P. Viallet, J. G. Hirschberg, A. W. Souter, C. Kohen, and B. Thorell, *Photochem. Photobiol.* **36**, 585 (1982).
4. A. Pradhan, P. Pal, G. Durocher, L. Villeneuve, A. Balassy, F. Babai, L. Gaboury, and L. Blanchard, *J. Photochem. Photobiol., B* **31**, 101 (1995).
5. Y. Wu and J. Y. Qu, *Opt. Lett.* **31**, 1833 (2006).
6. Y. Wu, P. Xi, J. Y. Qu, T. Cheung, and M. Yu, *Opt. Express* **12**, 3218 (2004).
7. Y. Wu, P. Xi, J. Y. Qu, T. Cheung, and M. Yu, *Opt. Express* **13**, 382 (2005).
8. R. N. Fichorova, J. G. Rheinwald, and D. J. Anderson, *Biol. Reprod.* **57**, 847 (1997).
9. N. D. Kirkpatrick, C. Zou, M. A. Brewer, W. R. Brands, R. A. Drezek, and U. Utzinger, *Photochem. Photobiol.* **81**, 125 (2005).
10. H. Schneckenburger and K. Konig, *Opt. Eng.* **31**, 1447 (1992).
11. K. Blinova, S. Carroll, S. Bose, A. V. Smirnov, J. I. Harvey, J. R. Knutson, and R. S. Balaban, *Biochemistry* **44**, 2585 (2005).
12. A. Gafni and L. Brand, *Biochemistry* **15**, 3165 (1976).
13. H. D. Vishwasrao, A. A. Heikal, K. A. Kasischke, and W. W. Webb, *J. Biol. Chem.* **280**, 25119 (2005).
14. D. K. Bird, L. Yan, K. M. Vrotsos, K. W. Eliceiri, E. M. Vaughan, P. J. Keely, J. G. White, and N. Ramanujam, *Cancer Res.* **65**, 8766 (2005).
15. A. C. Croce, A. Spano, D. Locatelli, S. Barni, L. Sciola, and G. Bottiroli, *Photochem. Photobiol.* **69**, 364 (1999).